LEGIBILITY NOTICE

A major purpose of the Technical Information Center is to provide the broadest dissemination possible of information contained in DOE's Research and Development Reports to business, industry, the academic community, and federal, state and local governments.

Although a small portion of this report is not reproducible, it is being made available to expedite the availability of information on the research discussed herein.

LA-UR -90-1897

CONF-9003166--1

Los Alamos National Laboratory is operated by the University of California for the United States Department of Energy under contract W-7405-ENG-36.

LA-UR--90-1997

DE90 011992

TITLE: Ilmenite Exsolution Schemes in Apollo-17 High-Ti Basalts

AUTHOR(S):
D. Vaniman, T. Muhich, G. Heiken

SUBMITTED TO: Proc. of the 21st Lunar and Planetary Sci. Conf.
Houston, Texas, March 1990

DISCLAIMER

Los Alamos Los Alamos National Laboratory
Los Alamos, New Mexico 87545

FORM NO 836 R4
ST NO 2629 5/91

MASTER

ILMENITE EXSOLUTION SCHEMES IN APOLLO-17 HIGH-TI BASALTS

L. Vaniman[1], T. Muhich[2], and G. Heiken[1]

[1]Los Alamos National Laboratory, Geology and Geochemistry, EES-1, Los Alamos, NM 87545

[2]Department of Geology, College of St. Thomas, St. Paul, MN 55105

ABSTRACT

Combined electron microprobe and scanning electron microscope (SEM) x-ray image analyses can be used to obtain semiquantitative data on the relations between ilmenite grains and their exsolved chromite and rutile. Comparisons of these data for ilmenites in four Apollo-17 high-Ti basalts with a database of electron microprobe analyses from the literature indicate that Cr expulsion from ilmenite can be as important (in some cases more important) as Fe^{2+} reduction in causing subsolidus exsolution of chromite and rutile from ilmenite.

INTRODUCTION

Exsolution features are common in lunar ilmenites, particularly in those that occur as rims around armalcolite (Haggerty et al., 1970) and many of those in coarse-grained high-Ti mare basalts. Haggerty et al. (1970) described exsolution lamellae of rutile, oriented along {012},

and lensoid rods of spinel, oriented along {001}, in ilmenites from the Apollo-11 high-Ti basalts. In a later study of similar exsolution features in Apollo-17 high-Ti basalts, Haggerty (1973) suggested that such exsolution features represent subsolidus reduction of Fe^{2+} in ilmenite to form rutile, chromite, and metallic Fe. Progressive reduction of mineral assemblages is evident throughout the crystallization and subsolidus cooling of lunar mare basalts and impact melts (El Goresy et al., 1972; BVSP, 1981).

There is considerable solid solution between ilmenite ($FeTiO_3$) and geikielite ($MgTiO_3$) in high-Ti mare basalts. There is no single, simple petrogenetic explanation for the variability in Mg contents of lunar ilmenites. Reaction with early-formed armalcolite appears to account for some of the highest MgO values (Haggerty, 1973), but high MgO contents may also occur where ilmenite grains are enclosed within Mg-rich olivines or pyroxenes (Warner et al., 1978). Our study of Mg variations in large ilmenite crystals from Apollo-17 high-Ti basalts (Muhich et al., 1990) showed that the Mg contents of exsolved ilmenite hosts correlate with the abundance of rutile + chromite exsolution. This observation lead us to suggest that the exsolution of rutile and chromite, which exclude Mg, causes the Mg concentration in the surrounding ilmenite to increase. A more critical examination leads us, in this paper, to reject this hypothesis.

The natural reduction of Fe^{2+} in lunar ilmenite, and its diminished Fe content through solid solution with $MgTiO_3$ or other constituents, are of interest in assessing the amount of reducible Fe^{2+} where ilmenite might be sought as an ore for oxygen production (McKay and Williams, 1979). The extractable oxygen in ilmenite is produced by reduction of

Fe^{2+} to Fe metal. There is therefore less extractable oxygen where Fe has been substituted by Mg, or where subsolidus reduction of Fe^{2+} has beaten the process plant to the once-available oxygen. Although these are at most second-order concerns among the ilmenites known to occur on the Moon with high Fe^{2+} content, it is important to address them for two reasons. First, a thorough understanding of ilmenite compositional variations is important in order to assess the feedstock requirements and the quantities and types of unoxidized slag that will result from lunar ilmenite reduction. Second, because of the potential problems in separating ilmenite from either soils or rocks (Vaniman and Heiken, 1990), it would be a tremendous boon to discover pre-concentrated ores of lunar ilmenite, such as possible (but unproven) cumulate pods that might be found in boulders excavated by impacts into exceptionally thick high-Ti lava flows. The value of such cumulate pods would be lost if it can be predicted that the ilmenites in them will have lost most of their Fe^{2+}, by reaction to rutile and Fe metal with oxygen loss, as they stewed in deuteric gases after they accumulated.

LITERATURE DATA

There is a large amount of published data on ilmenite compositions. Before examining the details of ilmenite compositional variation in a small subset of Apollo-17 basalt samples, it is useful to look at all the published analyses of high-Ti basalt ilmenites. In order to do this, we have compiled a database of 958 ilmenite analyses from 53 published sources. In examining this database critically, we found that only 56% (n=541) of the published analyses met our criteria for high-quality

electron microprobe analyses: a total weight % of oxides between 98%-101.25% and a total cation formula, based on 3 oxygens, between 1.985-2.010. Table 1 shows the statistical data for the 541 analyses selected from the literature. The complete data listing and a list of the references can be obtained by writing to the first author.

The selected subset of 541 ilmenite analyses indicates a broad range of Mg-Fe substitution (Fig. 1a), from 0 to 26% geikielite component with an average of 8.7% (in oxide weight proportions, this is 0 to 6.9% MgO, with an average of 2.3%). Higher Mg contents are cited in the literature (e.g., 8 wt% MgO in Haggerty, 1973, and 30% geikielite in Warner et al., 1978) but these occurrences are not documented by complete analyses. From the bulk of the published data, it is evident that such high-Mg ilmenites are rare. As a further caution in the use of Table 1, it should be noted that many authors publish only the extremes in composition to illustrate the range of compositions they determined. Nevertheless, the data in Table 1 represent a carefully screened survey of the available data.

The literature data show the expected strong negative correlation between Mg and Fe contents, reflecting the substitution of geikielite for ilmenite (Fig. 1a). There are no comparable correlations between Mg or Fe with Si, Zr, Al, Cr, or Mn; neither is there any significant correlation with R^{4+}, R^{3+}, or R^{2+} as groups. Part of this lack of minor-element correlation is due to the global nature of the data set, which includes analyses from ilmenite rims around armalcolite, from skeletal ilmenites in rapidly cooled basalts, from poikilitic ilmenites (overprinted by exsolution effects) in slowly cooled basalts, and from late-stage groundmass ilmenites and ilmenite rims. Each of these

associations will provide minor-element data reflecting a different origin, resulting in a mixture of ilmenite compositional types within the database. This cause of variation is discussed briefly in terms of Cr content at the end of this paper.

The main use of the literature data compiled here (Table 1) is to define the compositional range of common ilmenite types. It also provides a template against which the ilmenite compositions in single samples can be compared.

METHODS

Four basalts from the Apollo 17 site were selected for analysis of ilmenite compositions, sizes, and shapes. Two of these basalts are coarse-grained (thin sections 70035,14 and 78505,67), one is medium-grained (71055,66), and one is fine-grained (70215,89). The two coarse-grained samples were also analyzed by scanning electron microscope (SEM) energy-dispersive image analysis to measure the extent of rutile and chromite exsolution.

Electron microprobe data were collected for comparison with the literature analyses and to investigate the relations of crystal composition to size, shape, and extent of exsolution. A Cameca CAMEBAX microprobe was used, operated at 15 kV with a beam current of 15 nA. Multiple analyses (3 to 15) were made within each ilmenite grain analyzed by microprobe.

Backscattered-electron images were collected with an ISI DS-130 scanning electron microscope. Energy-dispersive x-ray maps of individual ilmenite grains were also obtained, using the Tracor Northern image-

analysis program VISTA to map distributions and abundances of rutile and chromite lamellae within 128x128-pixel images. All images were collected at 19 kV. Magnification was varied with crystal size. X-ray detection of exsolution features depends on the width of the lamellae; lamellae thinner than ~2 μm are generally too thin to be detected, but studies with backscattered electron images indicate few lamellae with widths less than 4 μm. It is possible, however, that submicroscopic features may have gone undetected. Multiple determinations of chromite and rutile abundances in different areas of large single ilmenite crystals indicate a relative error of ±20% in these determinations. Most of the ilmenite-grain size and shape data analyzed here are from Heiken and Vaniman (1990); additional data correlated specifically with the electron microprobe data were collected from photographs with a planimeter.

ILMENITE SIZE DISTRIBUTIONS AND COMPOSITIONS

Figure 2 shows the cumulative distribution of ilmenite grains, ranked by grain width, in the four basalts studied. The total volume percentage of ilmenite in these samples ranges from 14% to more than 19%; data in Fig. 2 are arranged such that the largest (i.e., widest) grains are at the bottom of the figure, and successively smaller grains are added to each curve to produce the total ilmenite volume in each sample.

Note that although many grains (143 to 372) were measured in each sample (Table 2), more than half of the total volume of ilmenite in each sample is accounted for by the widest crystals (the largest 4% to 10% of the grains measured). Moreover, even though the grain-width curves for

the two coarsest samples, 78505 and 70035, seem to overlap, the average ilmenite grain width in basalt 70035 is much lower because there are many more small crystals in this sample (at the upper end of the curve) than in basalt 78505. This difference can be seen by comparing the data in Table 2 on average grain width (which is much lower in basalt 70035) with data on the ilmenite width at 50% of the total ilmenite volume, which is essentially the same (345-380 μm) in each sample.

Ilmenite sizes were compared with the compositional variations between grains. Compositional data for ilmenites from the four basalts studied are summarized in Table 2. No correlation could be found in any sample between chemical variables and grain size. The smallest grains of ilmenite have Mg-Fe compositional ranges similar to the largest grains.

Figure 1b and 1c compare the Mg-Fe compositional ranges of ilmenites in the four basalts analyzed. Data for basalts 78505, 71055, and 70215 are compiled in Fig. 1b. In this figure, only the data points for basalt 78505 are shown; data for the medium-grained basalt 71055 and the fine-grained basalt 70215 overlap along the same Mg-Fe exchange trend, so their data points are omitted and instead, their compositional ranges are indicated by arrows. There is no hiatus in composition within the compositional ranges of the medium-grained and fine-grained basalts (71055, 70215), whereas the compositional data for coarse-grained basalts 78505 (Fig. 1b) and 70035 (Fig. 1c) fall into two or three compositional clusters.

Overall, the compositional ranges within some single basalt samples are large enough to represent a large fraction of all analyses from all samples cited in the literature. The Mg-Fe compositional range in basalt 71055 alone is 65% of the full literature range. Our main interest,

however, is the apparent clustering of ilmenite compositional groups within the two coarse-grained basalts (samples 78505 and 70035).

SEM ANALYSIS OF EXSOLUTION FEATURES

Energy-dispersive image analysis was used to map the volume percentages of chromite and ilmenite exsolution features in the two coarse basalts, 78505 and 70035. The results of this mapping are summarized in Tables 3 and 4. In each table, the ilmenite grains mapped are divided into Mg-content groups: high-Mg, medium-Mg, and low-Mg for basalt 70035 in Table 3 (corresponding to the three compositional clusters seen in Fig. 1c); high-Mg and low-Mg for basalt 78505 in Table 4 (corresponding to the two compositional clusters seen in Fig. 1b).

Basalt 70035 (Table 3) shows a good correlation between the abundances of both chromite and rutile lamellae, and the Mg content of the exsolved ilmenite host. There appears to be a comparable correlation between rutile abundance and Mg content of the host ilmenite in basalt 78505, but in this sample the correlation with chromite content is not as prominent. Possible causes of a correlation between Mg content of the host crystal and the abundance of exsolved rutile or chromite are considered below.

DISCUSSION: EXSOLUTION SCHEMES

The causes of exsolution in ilmenites of the coarse-grained high-Ti lunar basalts are related to the abundances of exsolved chromite and rutile, the relative proportions of exsolved chromite and rutile, the

original composition of the unexsolved ilmenite, and the final composition of the host ilmenite. These factors are considered in Table 5, where two different exsolution schemes are outlined, one that produces rutile alone, and another that produces chromite as well as rutile.

Reduction-driven Exsolution.

The reaction which produces rutile alone is driven by reduction of the Fe^{2+} in ilmenite (Table 5, Reaction 1). The evidence for progressive reduction during the cooling of lunar basalts is compelling (fayalite and ulvospinel reduction; El Goresy et al., 1972). The exsolution of rutile with loss of oxygen (and Fe metal) from original ilmenite is one of the observations that has been used to establish the importance of such reduction (Haggerty, 1973). None of the minor constituents in ilmenite, including $MgTiO_3$ (geikielite), are involved in this reduction. If carried to extremes, it is conceivable that the geikielite component could be highly concentrated in the remaining ilmenite, producing, in the most extreme cases, an intergrowth of geikielite and rutile.

It is intuitive that the oxygen produced in ilmenite Fe^{2+} reduction will be lost, but it is less obvious that the Fe metal will be expelled as well. The expulsion of Fe metal in this process has, however, been known for some time, based on the observations of Fe metal and troilite occurring around grain boundaries and within fractures of exsolved ilmenites (El Goresy and Ramdohr, 1975). Recent experiments on the reduction of ilmenite grains (to produce oxygen as a lunar resource) have confirmed that semimolten Fe metal migrates outward, against the direction of reductant gas (CO, hydrogen) transport into the grain

(SERC, 1990). This research demonstrates that, in fact, the slow migration of the Fe metal is the rate-limiting step in ilmenite reduction.

Complete reaction of ilmenite tc rutile, with expulsion of Fe and oxygen, results in a large loss in volume from the original ilmenite grain (41%; Table 5). However, the volume percent of rutile lamellae within exsolved ilmenites is small (<2%; Tables 3 and 4), and much of the rutile present appears to be derived by another reaction, described below, in which there is essentially no volume loss to the original ilmenite.

Thermally-driven Exsolution.

Chromium in ilmenite is not involved in exsolution by reduction, unless it is reduced from Cr_2O_3 to CrO. There is evidence for partial reduction of Cr^{3+} to Cr^{2+} in some lunar basalts, but analyses indicate that the chromite exsolution lamellae in ilmenites are largely $FeCr_2O_4$, rather than $Cr^{2+}(Cr^{3+})_2O_4$ (the chromite lamellae do, however, appear to have a significant component of $FeAl_2O_4$; apparently the R^{3+} cations are readily expelled from the ilmenite structure of alternating R^{2+}-R^{4+} cation layers). Treating essentially all Cr in ilmenite and its exsolution features as Cr^{3+} fits the observed mineralogy. Exsolution of chromite from ilmenite is therefore not caused by reduction of Cr^{3+}, leading to the conclusion that this exsolution is instead caused by re-equilibration at temperatures lower than those at which the ilmenite grains originally formed.

Reaction 2 in Table 5 is based on an "ideal" chromian ilmenite component, $CrCrO_3$, which must react with an equivalent ilmenite formula

unit to produce one formula unit each of chromite and rutile. In volume proportions, these exsolution products occur with a rutile/(rutile + chromite) volume ratio of 0.30. There is essentially no volume loss in this exsolution scheme.

Mixed-origin Exsolution.

From Table 5, it is evident that purely reduction-driven ilmenite exsolution should result in a rutile/(rutile + chromite) ratio of 1.00, whereas in thermally-driven chromite exsolution this ratio should be 0.30. The actual rutile/(rutile + chromite) ratios in Tables 3 and 4 range from 0.22 to 0.90. The values below 0.30 are allowed for by our estimated relative errors of ±20% in reproducibility of rutile and chromite abundance measurements. The small percentages of the exsolution features being measured, plus the effects of inhomogeneous exsolution distributions within grains along with variable grain orientations, make such large errors inevitable. Nevertheless, the rutile/(rutile + chromite) data in Tables 3 and 4 are sufficient to suggest that the predominant exsolution scheme in ilmenites of basalt 70035 is thermally driven (reaction 2, Table 5), whereas the exsolution in ilmenites of basalt 78505 is mixed (reduction- and thermally-driven).

It would be of value to develop this exsolution-feature measurement technique as a quantitative measure of ilmenite reduction in lunar basalts, but the small percentages of exsolution involved make this development problematical. Although an energy-dispersive x-ray map at 128x128 pixels provides 16 measurements per 0.1% of area, the problems of grain variability and orientation are not easily overcome. This approach is useful, however, for semiquantitative comparisons between

basalts and for a general evaluation of the relative importance of different schemes of ilmenite exsolution.

CONCLUSIONS

The exsolution schemes observed in ilmenites of Apollo-17 high-Ti basalts lead to the following conclusions.

Exsolution of Mg-free Rutile and Chromite does not Significantly Increase the Mg Content of the Host Ilmenite.

In contrast to our earlier suggestions (Muhich et al., 1990), exsolution of Mg-free phases is not a significant factor in altering the Mg content of the surrounding ilmenite. If this were the case, then it should be possible to reduce the spread of exsolved ilmenite compositions (Fig. 1b,c) to a single unexsolved ilmenite composition with low Mg content. That is, by recombining the host and lamellae compositions, the high- and medium-Mg clusters in Fig. 1b,c should collapse toward the Fe axis and toward the low-Mg compositional clusters. In fact, the recombined estimates of unexsolved ilmenite Mg-Fe compositions differ little from those of the exsolved grains (Fig. 3). Apparently the ilmenite Fe-Mg compositional clusters within basalt samples are due to primary igneous effects and not to subsolidus exsolution.

Chromium Content is a Key Factor in Determining the Extent of Subsolidus Ilmenite Exsolution.

In Table 3 (basalt 70035), the Mg content of the exsolved ilmenites correlates well with the volumes of chromite and rutile exsolved. This correlation is less evident in Table 4 (basalt 78505), but here it appears that the exsolution is driven by mixed reduction and thermal schemes, rather than being predominantly due to expulsion of Cr from ilmenite on cooling, as in basalt 70035 (Table 3). As noted above, the correlation of Mg content with degree of exsolution is a result of each original ilmenite grain's Mg content, rather than a product of the exsolution process. Indeed, although the Cr contents vary little between the high-Mg to low-Mg exsolved ilmenites, the reconstructed original ilmenite grains do show a good correlation between Mg and Cr content, due to the contribution of large amounts of Cr even from the small volumes of chromite recombined. The abundance of rutile exsolution also correlates with the ilmenite Mg and Cr content, because rutile is a necessary byproduct of Cr expulsion from ilmenite (reaction 2, Table 5).

It might be expected that the literature data on ilmenites would show some evidence of the importance of Cr in driving ilmenite exsolution, and indeed this appears to be the case. Figure 4 shows the covariation of Cr and Mg in the 484 literature data on high-Ti basalt ilmenites described above that include analyses for Cr (Table 1). Below Mg contents of 0.10 per 3-oxygen formula unit, there is a good correlation between Cr and Mg. Above this value, the Cr contents of ilmenites "plateau" at about 0.015 cations per 3-oxygen formula unit. This is the same Cr content observed in the exsolved ilmenite grains within the basalts studied here (Table 2), and we interpret this to

indicate a common compositional limit to the Cr contents of exsolved ilmenites in lunar basalts. This limit is probably determined by a relatively constant temperature (below 830°C; El Goresy and Ramdohr, 1975) of ilmenite exsolution and compositional re-equilibration within cooling high-Ti mare basalts.

ACKNOWLEDGEMENTS

This study was supported by the U.S. Department of Energy's Science and Engineering Research Semester (SERS) Program and by the National Aeronautics and Space Administration. A review by D. Bish helped to improve the text and contents.

REFERENCES

Brown G.M., Emeleus C.H., Holland J.G., and Phillips R. (1970) Mineralogical, chemical and petrological features of Apollo 11 rocks and their relationship to igneous processes. Proc. Lunar Sci. Conf. 1st, pp. 195-219.

BVSP (Basaltic Volcanism Study Project) (1981) Basaltic Volcanism on the Terrestrial Planets. Pergamon Press, NY, 1286 pp.

El Goresy A. and Ramdohr P. (1975) Subsolidus reduction of lunar opaque oxides: Textures, assemblages, geochemistry, and evidence for a late-stage endogenous gas mixture. Proc. Lunar Sci. Conf. 6th, pp. 729-745.

El Goresy A., Taylor L.A., and Ramdohr P. (1972) Fra Mauro crystalline rocks: Mineralogy, geochemistry and subsolidus reduction of the opaque minerals. Proc. Lunar Sci. Conf. 3rd, pp. 333-349.

Haggerty S.E. (1973) Apollo 17: armalcolite paragenesis and subsolidus reduction of chromian-ulvospinel and chromian-picroilmenite. EOS 54, 593-594.

Haggerty S.E., Boyd F.R., Bell P.M., Finger L.W., and Bryan W.B. (1970) Opaque minerals and olivine in lavas and breccias from Mare Tranquillitatis. Proc. Lunar Sci. Conf. 1st, pp. 513-538.

Heiken G.H. and Vaniman D.T. (1990) Characterization of lunar ilmenite resources. Proc. Lunar Planet. Sci. Conf. 20th, pp. 239-247.

McKay D.S. and Williams R.J. (1979) A geologic assessment of potential lunar ores. NASA SP-428, pp. 243-256.

Muhich T., Vaniman D., and Heiken G. (1990) Ilmenite in high-Ti Apollo 17 basalts: Variations in composition with degree of exsolution. In Lunar and Planetary Science XXI, pp. 817-818. Lunar and Planetary Institute, Houston.

SERC (Space Engineering Research Center) (1990) Ilmenite reaction mechanisms and kinetics probed. The SERC Newsletter, Univ. of Arizona, Tucson. Vol. 1, No. 2, pp. 4-6.

Vaniman D.T. and Heiken G.H. (1990) Getting lunar ilmenite: From soils or rocks? In Engineering, Construction, and Operations in Space II (S.W. Johnson and J.P. Wetzel, eds.). Proc. Space 90, pp. 107-116.

Warner R.D., Nehru C.E., and Keil K. (1978) Opaque oxide mineral crystallization in lunar high-titanium mare basalts. Amer. Miner. 63, 1208-1224.

Table 1: Literature Data on Ilmenites from 541 Apollo-11 and Apollo-17 High-Ti Basalts

statistics for oxide weight percent data

	mean	median	maximum	minimum	std.dev.	skewness	kurtosis	number
SiO_2	0.36	0.30	1.09	0.00	0.26	0.62	-0.59	356
TiO_2	52.4	52.4	53.3	51.0	0.46	-0.26	-0.37	541
ZrO_2	0.14	0.09	0.54	0.00	0.11	1.30	1.14	226
Al_2O_3	0.20	0.17	1.24	0.00	0.18	2.34	7.73	366
Cr_2O_3	0.62	0.63	2.11	0.01	0.23	0.35	3.92	484
FeO	43.3	43.6	48.2	35.0	2.5	-0.72	0.61	541
MnO	0.46	0.47	0.67	0.15	0.08	-0.98	1.80	433
MgO	2.33	2.23	6.92	0.00	1.44	0.85	0.70	534

statistics for cation formulae, based on 3 oxygens

	mean	median	maximum	minimum	std.dev.	skewness	kurtosis	number
Si	0.009	0.007	0.027	0.000	0.006	0.62	-0.59	356
Ti	0.983	0.983	1.001	0.957	0.009	-0.26	-0.37	541
Zr	0.002	0.001	0.007	0.000	0.001	1.30	1.14	226
Al	0.006	0.005	0.036	0.000	0.005	2.34	7.73	366
Cr	0.012	0.012	0.042	0.000	0.004	0.35	3.92	484
Fe	0.905	0.910	1.005	0.730	0.053	-0.72	0.61	541
Mn	0.010	0.010	0.014	0.003	0.002	-0.98	1.80	433
Mg	0.087	0.083	0.257	0.000	0.054	0.85	0.70	534

Table 2: Average Compositions and Grain Width Parameters of Ilmenites in Four High-Ti Basalts (std. dev. in parentheses)

sample:	78505	71055	70215	70035
	Weight Percent Oxides			
SiO_2	0.03(.02)	0.01(.03)	0.13(.23)	0.01(.01)
TiO_2	53.4 (.8)	53.3 (.6)	52.5 (.5)	53.4 (.6)
ZrO_2	0.11(.12)	0.03(.04)	0.05(.02)	0.08(.11)
Al_2O_3	0.04(.03)	0.08(.04)	0.11(.06)	0.04(.02)
Cr_2O_3	0.77(.17)	0.64(.10)	0.82(.17)	0.80(.13)
FeO	42.0 (1.7)	43.1 (.8)	43.7 (.7)	42.7 (1.2)
MnO	0.37(.06)	0.45(.06)	0.45(.06)	0.37(.04)
MgO	3.37(1.22)	2.80(.50)	2.33(.46)	2.96(.87)
Σ	100.1	100.4	100.1	100.4
	cations based on 3 oxygens			
Si	0.001(.001)	0.000(.001)	0.003(.006)	0.000(.000)
Ti	0.988(.005)	0.988(.005)	0.980(.007)	0.989(.006)
Zr	0.001(.001)	0.000(.000)	0.001(.000)	0.001(.001)
Al	0.001(.001)	0.002(.001)	0.003(.002)	0.001(.001)
Cr	0.015(.003)	0.012(.002)	0.016(.003)	0.015(.003)
Fe	0.864(.023)	0.888(.021)	0.907(.018)	0.879(.032)
Mn	0.008(.001)	0.009(.001)	0.009(.001)	0.008(.001)
Mg	0.123(.044)	0.103(.018)	0.086(.017)	0.108(.031)
Σ	2.001	2.002	2.005	2.001
# of anal.	79	66	11	31
av. grain width (μm):	132(142)	47(64)	17(19)	53(101)
grain width at 50% total ilmenite volume (μm):	380	182	59	345
# measured:	128	318	143	372

Table 3: Chromite and Rutile Lamellae in Ilmenites of 70035

	mol% $MgTiO_3$ in exsolved ilmenite	vol% chromite	vol% rutile	ratio of rutile to (rutile + chromite)
High-Mg Ilmenites:				
L4	$0.149 \pm .004$	2.8	1.4	.33
L7	$0.154 \pm .002$	2.6	1.6	.38
Medium-Mg Ilmenites:				
L1	$0.103 \pm .001$	1.5	0.8	.35
L2	$0.105 \pm .002$	1.9	1.1	.37
L3	$0.114 \pm .004$	1.2	0.8	.40
M2	$0.114 \pm .003$	1.9	0.9	.33
Low-Mg Ilmenites:				
L5	$0.068 \pm .002$	0.7	0.3	.30
L8	$0.080 \pm .003$	0.7	0.2	.22

Correlation coefficients: between $MgTiO_3$ and chromite, R=0.94
between $MgTiO_3$ and rutile, R=0.95

Table 4: Chromite and Rutile Lamellae in Ilmenites of 78505

	mol% $MgTiO_3$ in exsolved ilmenite	vol% chromite	vol% rutile	ratio of rutile to (rutile + chromite)
High-Mg Ilmenites:				
L1	0.165±.004	2.1	1.6	.43
M1	0.144±.004	4.3	1.9	.31
M3	0.175±.002	1.4	2.1	.60
Low-Mg Ilmenites:				
L2	0.102±.004	2.1	1.8	.46
L3	0.085±.003	1.6	0.5	.24
L4	0.058±.001	0.1	0.9	.90
M2	0.053±.004	0.6	0.2	.25

Correlation coefficients: between $MgTiO_3$ and chromite, R=0.58
between $MgTiO_3$ and rutile, R=0.84

Table 5: Ilmenite Exsolution Schemes

	reaction	vol. ratio of rutile to (rutile + chromite)	Δvolume with Fe_2O loss*
1) Reduction Driven	$FeTiO_3 \rightarrow TiO_2 + Fe + O\uparrow$	1.00	-41%
2) Thermally Driven	$FeTiO_3 + CrCrO_3 \rightarrow FeCr_2O_4 + TiO_2$	0.30	- 0.7%
3) Mixed Origin	$2FeTiO_3 + CrCrO_3 \rightarrow FeCr_2O_4 + 2TiO_2 + Fe + O\uparrow$	0.46	-12%

*This column is calculated with the assumption that all Fe and O are expelled from the original ilmenite grain, as observed in exsolved ilmenites from high-Ti basalts. Volumes used in these calculations are: chromite, 73.5 A^3 per $FeCr_2O_4$; rutile, 31.0 A^3 per TiO_2; "chromian" ilmenite, 48.3 A^3 per $CrCrO_3$; ilmenite, 52.6 A^3 per $FeTiO_3$.

FIGURE CAPTIONS

Fig. 1. Plots of Mg vs. Fe contents in ilmenites, showing the number of cations per 3-oxygen formula unit. Data in (a) are from 534 ilmenite analyses published in the literature. Data in (b) show ilmenites from coarse-grained basalt 78505, compared with the compositional ranges in medium-grained basalt 71055 and fine-grained basalt 70215 (data points from these latter two basalts would plot on top of those from basalt 78505 and are therefore omitted). Note the two compositional clusters (high-Mg and low-Mg) for ilmenite analyses from basalt 78505. Data in (c) are from coarse-grained basalt 70035 (note the three compositional clusters, high-Mg, medium-Mg, and low-Mg).

Fig. 2. Plots of grain width vs. volume percent of ilmenite in basalts 78505, 70035, 71055, and 70215. Each curve is configured so that the largest grain width in each sample is plotted on the x axis, with successively smaller grains added above along cumulative growth curves that reach the total ilmenite content for each sample, plotted on the y axis.

Fig. 3. Reconstructed ilmenite compositions in basalt 70035, based on the data in Fig. 1c and in Table 3. Axes indicate cations per 3-oxygen formula unit. Ellipses represent the three compositional groups of high-Mg, medium-Mg, and low-Mg exsolved ilmenites in Fig. 1c; crosses show the reconstructed original ilmenite compositions determined by recombining the exsolved volumes of chromite, rutile, Fe metal, and oxygen into the host ilmenite. Note that the reconstructed original ilmenites differ little from the exsolved ilmenites in Mg-Fe composition.

Fig. 4. Variation between Cr and Mg in 484 ilmenite analyses from the literature. Axes show compositions in terms of cations per 3-oxygen formula unit. The sample with very high Cr content is from basalt 10017 (Brown et al., 1970). There is a general correlation between Cr and Mg at Mg contents below 0.10 cations per formula unit; above this Mg content, the Cr content "plateaus" at ~0.015 cations per formula unit, possibly indicating the general Cr content for ilmenites equilibrated with exsolved chromite on cooling of high-Ti lunar basalts.

Fig. 1

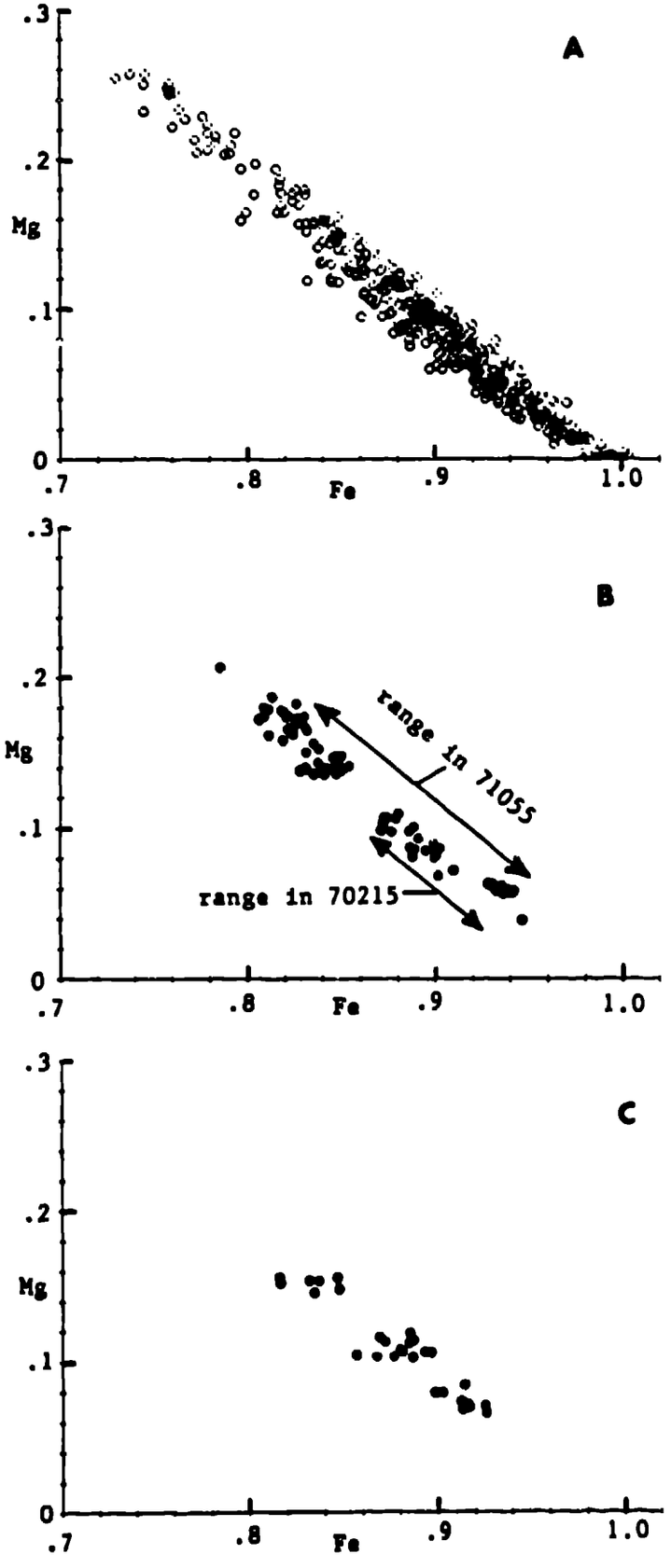

Fig. 2

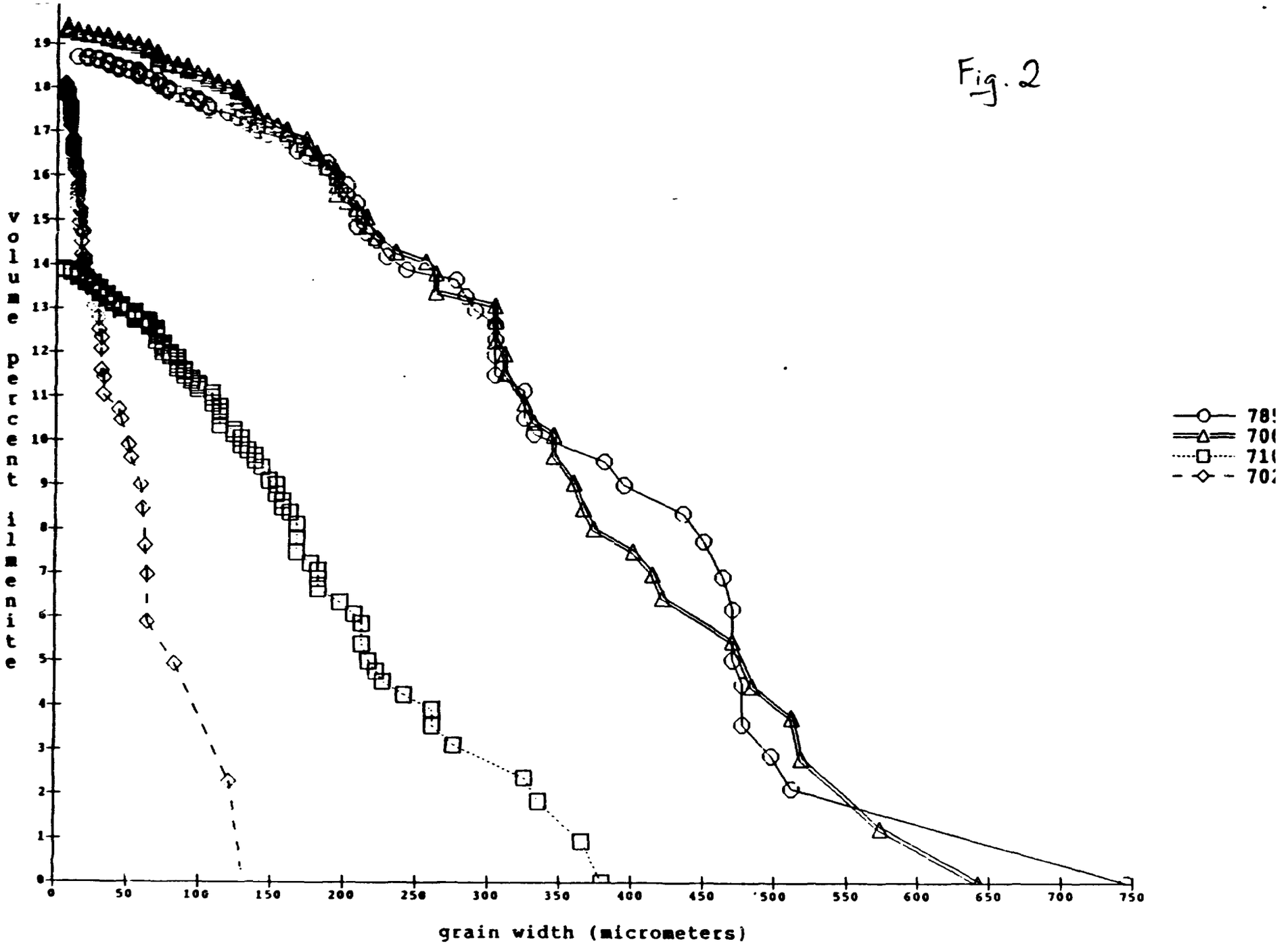
volume percent ilmenite
0
1
2
3
4
5
6
7
8
9
10
11
12
13
14
15
16
17
18
19
0
50
100
150
200
250
300
350
400
450
500
550
600
650
700
750
grain width (micrometers)
78
70
71
70

Fig. 3

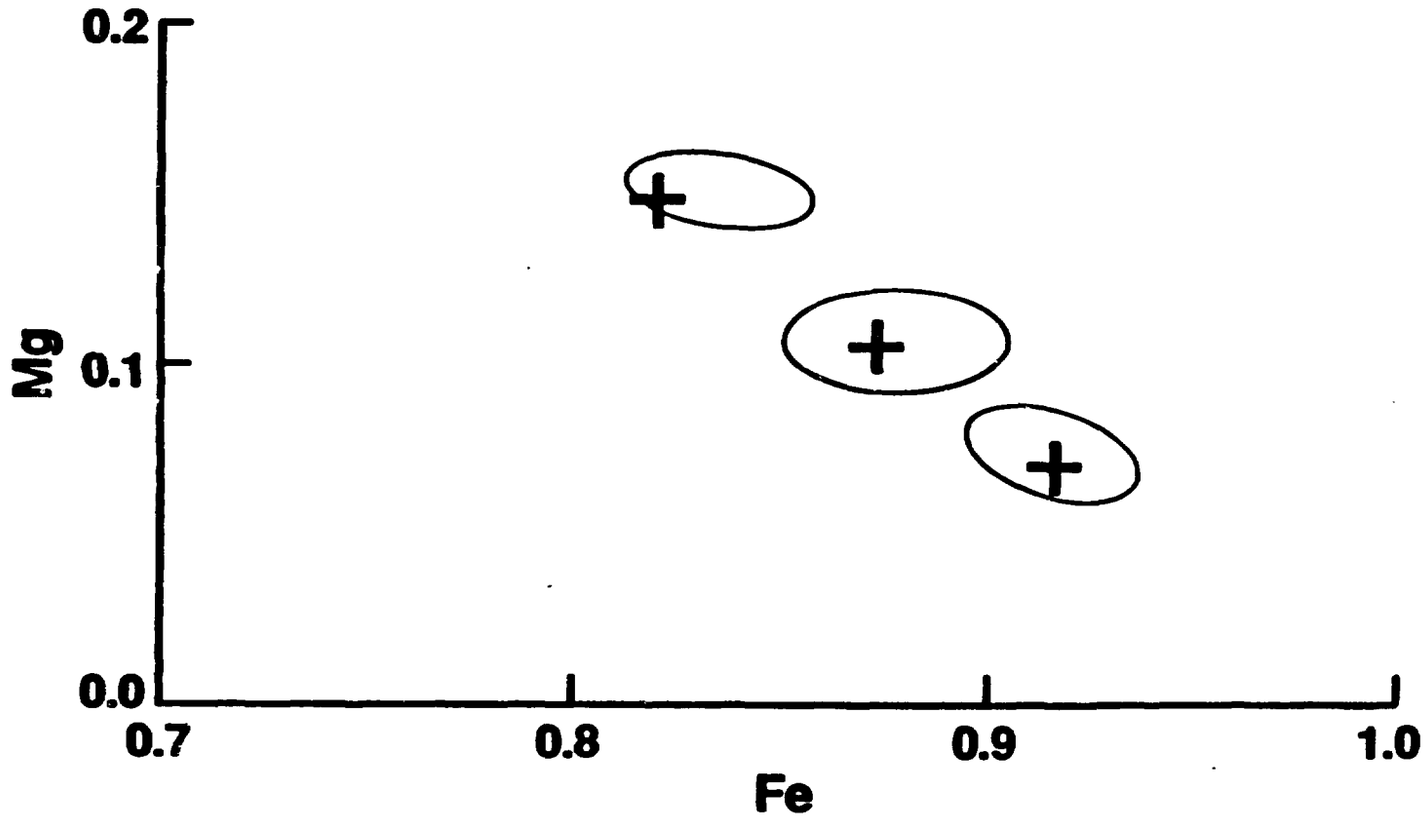

Fig. 4

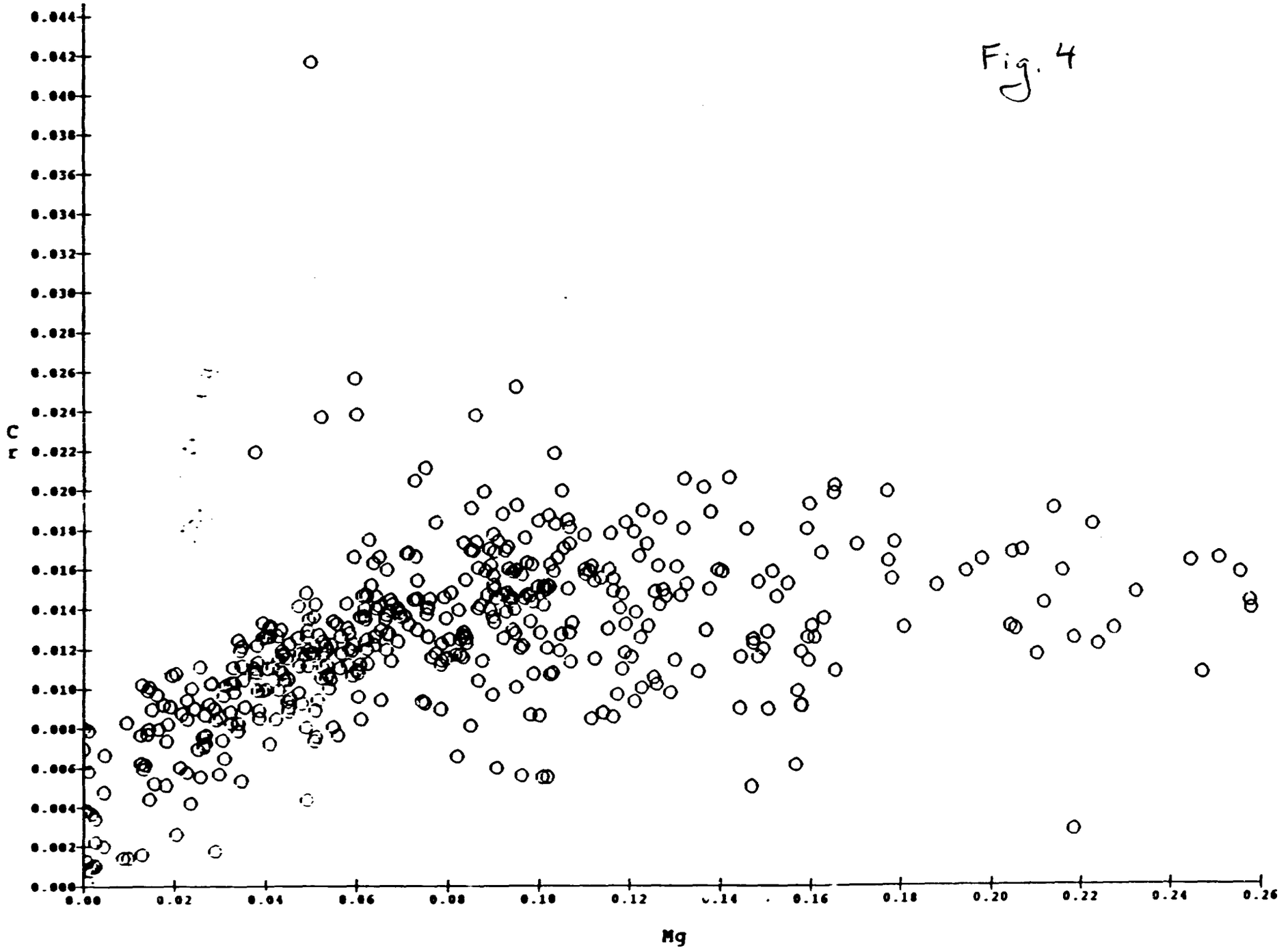
0.044
0.042
0.040
0.038
0.036
0.034
0.032
0.030
0.028
0.026
0.024
0.022
0.020
0.018
0.016
0.014
0.012
0.010
0.008
0.006
0.004
0.002
0.000
C
r
0.00
0.02
0.04
0.06
0.08
0.10
0.12
0.14
0.16
0.18
0.20
0.22
0.24
0.26
Mg